Scientific Research Publishing

World Journal of Mechanics, 2024, 14, 185-198
https://www.scirp.org/journal/wjm
ISSN Online: 2160-0503
ISSN Print: 2160-049X

Improving Energy Efficiency of Tunnel Furnace by Using Heat Optimization Model

Arup Mallick[1], Subir Banerjee[1], Ranjay Kumar Singh[2], P. N. Shivangi[2], Pinder Singh Mandley[1], Biswajit Ghosh[1], Chaitanya Bhanu[2], Mrityunjay Kumar Singh[1]

[1]Product Technology, Tata Steel, Mumbai, India
[2]LD & Thin Slab Caster, Tata Steel, Mumbai, India
Email: arup.mallick@tatasteel.com

How to cite this paper: Mallick, A., Banerjee, S., Singh, R.K., Shivangi, P.N., Mandley, P.S., Ghosh, B., Bhanu, C. and Singh, M.K. (2024) Improving Energy Efficiency of Tunnel Furnace by Using Heat Optimization Model. *World Journal of Mechanics*, **14**, 185-198.
https://doi.org/10.4236/wjm.2024.149009

Received: September 1, 2024
Accepted: September 27, 2024
Published: September 30, 2024

Abstract

Reheating furnace of an integrated steel plant consumes intensive fuel as input energy to heat up stocks prior to hot rolling process. In current scenario, the elevated cost of productivity due to increasing fuel price is emerging as a key concern for the steel industry. A continuous improvement in reduction of fuel consumption is one of the key objectives for the manufacturing units. Numerous research work is going on worldwide to increase the energy efficiency of reheating furnaces. Computational Fluid Dynamics (CFD) and numerical modelling are mostly being used for predicting thermal and reactive fluid characteristic inside a furnace. However, the said methods are very expensive and require a huge infrastructure to compute the results. In addition, these results are not available on real time basis to take corrective action due to high computational time. In this article, an alternative approach has been adopted where complete heat and mass balance of entire tunnel type reheating furnace has been carried out. This study includes first principle-based model where heat conduction, convection and radiation with combustion reactions of the fuel components have been considered. Based on these theoretical calculations, the model is used to identify heat losses at various locations of the furnace. Moreover, a method to optimize the mixing ratio of air and fuel (mixed gas) along with monitoring of heat recovery from combined recuperator have been covered. Based on the model outcome, a significant improvement in furnace efficiency has been achieved, leading to reduction in fuel consumption in the range of 12%.

Keywords

Heat Balance, Energy Efficiency, Reheating Furnace, Fuel Consumption,

Air-Fuel Ratio

1. Introduction

In steel plant, reheating furnaces are commonly used after continuous slab casting process for reheating slabs to keep the slab temperature at or above a critical temperature for hot rolling operation. Reduction of energy consumption by reducing the fuel consumption have attracted attention to many researchers. Numerous research articles have been published on the same subject. There is a consensus among researchers that the reduction in productivity cost at elevated fuel price is a key challenge. In addition, product quality is a key parameter which has a direct relation to the slab exit temperature, which determines the quality of hot rolled product. Therefore, compromising product quality with reduced energy consumption is highly non-desirable. Hence, an optimized method of heat distribution is required where a complete heat loss analysis at various parts of a reheating furnace is to be considered. Jang *et al.* [1] has explained the various numerical models and methods developed in recent past and these models can be broadly classified into two categories. First one is Computational Fluid Dynamics (CFD) based numerical models which predict the thermal and reactive fluid characteristic used for slab heating. This method is computationally very expensive and requires expensive infrastructure [2]-[8]. The second one is comparatively simple where model is based on analysis of radiative heat transfer inside the furnace and transient heat conduction within the slab [9]-[11]. Overall, the published articles have focused on minimization of energy based on optimization of slab heating pattern. The optimization methods such as simplified conjugate-gradient method (SCGM) and shooting method have been extensively used as an optimizer to search for optimum temperature for preheating zone, heating zone and soaking zone. Optimization of residence time for a slab or billet is another way to minimize unnecessary fuel consumption. This method can also reduce the chance of thicker scale formation on the slab or billet surface. Han *et al.* [12] has analyzed optimal residence time of a slab using numerical simulation of a reheating furnace. The authors have considered two criteria which are emission temperature and uniformity. Based on these, five residence time cases were investigated, and the analysis showed that 7427 sec. was the most optimum residence time for a slab inside the reheating furnace.

All the above studies, based on CFD and numerical models with various assumptions may partially be efficient for achieving the desired goal of reduction in fuel consumption. However, variation in furnace dimension, combusting characteristics of fuel, calorific value of input energy do not allow parallel and quick deployment of the said models. Current investigation focuses on finding an alternative and generalized method that can optimize input energy in a very efficient way. This method also ensures that the model can be horizontally deployed for various types of reheating furnaces. In this present study, a method has been described for

optimizing fuel consumption of a continuous tunnel furnace (Figure 1). The characterization of combusting mixed gas has been carried out and based on analysis results, heat and mass balance of entire furnace has been studied. Typically, the efficiency or rate of combustion of a mixed gas depends on the mixing composition, percentage of gas mixing, including oxygen availability, temperature, and pressure of the mixed gas [13]. In recent study of Lee *et al*. [14], authors have carried out an efficiency analysis for air-fuel and oxy-fuel of different mixing percentage for a reheating furnace. In total 5 cases, 2 for air-fuels and 3 for oxy-fuel performances have been analyzed. Here, they have found oxy-fuel has the potential of 50% enhancement in efficiency compared to air-fuel combustion. However, in this present study the energy optimization experiment has been conducted based on air-fuel combustion technique.

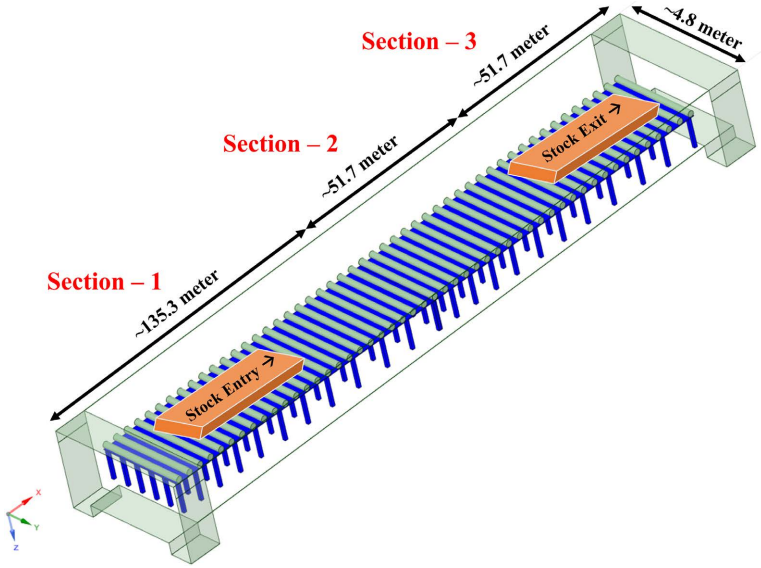

Figure 1. Schematic of tunnel type continuous furnace.

2. Analysis and Model Development

2.1. Furnace Dimension and Operation Details

In this work, slab-heating process by two tunnel furnaces of Tata Steel Ltd. India [Furnace A and Furnace B] at continuous thin slab caster and rolling has been considered. The slab heating is carried out at both the furnaces by air-fuel combustion. The length of each furnace is approximately 239 meter (Figure 1) and "Furnace B" has swivel over operation technique where, slabs are shifted from furnace B to furnace A, for uninterrupted slab feeding facilities to a single hot rolling operation line (Figure 2). The objective of this roller base tunnel type continuous furnace is to maintain desired rolling temperature throughout the furnace length. It also enables continuous operation of slab heating for uninterrupted rolling operation. The slab entry temperature into tunnel type furnace varies between 900˚C - 950˚C whereas, slab exit temperature is commonly between 1100˚C - 1150˚C for both the furnaces. It indicates, required heat or energy input should

be between 12% - 18% of total heat input for achieving desired slab out temperature from the furnace. The entire furnace is divided into several zones which are namely Zone1 to Zone9 for furnace A and Zone1 to Zone8 for furnace B. Each zone consists of three thermocouples (TC) in alternative furnace walls (Figure 3). In order to operate such a huge furnace, these zones are combinedly divided into three virtual sections for both the furnaces *i.e.*, for furnace A: Zone1 to Zone3 are considered as Section1, Zone4 to Zone7 are considered as Section2 and Zone8 to Zone9 are considered as Section3. Similarly, for furnace B: Zone1 to Zone3 are considered as Section1, Zone4 to Zone7 are considered as Section2 and Zone8 is considered as Section3. Three recuperators are attached with the three sections respectively of each furnace for recovering the heat from exiting flue gas, which is predominantly used as recycled heat input into the furnace. Both the furnaces are operating on roller base for pushing stocks from charging to discharging point through the furnace. There are 218 rolls in Furnace-A and 214 rolls for Furnace-B, which are embedded with refractory and continuously cooled by inflow of water. The temperature range for inlet water is in the range of 250˚C to 350˚C.

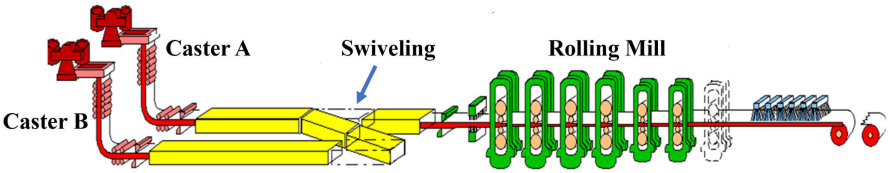

Figure 2. Swiveling operation of furnace.

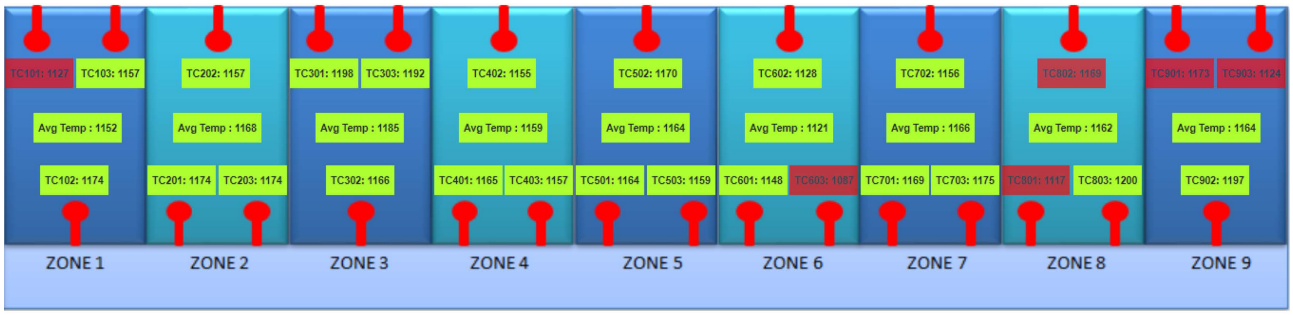

Figure 3. Zone wise thermocouple position.

2.2. Combustion Analysis of Mixed Gas

In an integrated steel plant, mixed gas is commonly used as combustion agent where byproduct gases from coke oven, blast furnace and Linz-Donawitz furnace (LD) are mixed with a proportion based on availability. Zheng *et al.* [15] has suggested an optimized model for the users of byproduct gas, considering fluctuation in Calorific Value (CV) and supply patterns. Authors have explained the various reasons for inconsistent CV of mixed gas. Hence, instantaneous variation in CV requires dynamic analysis of mixed gas composition at an every instance before combustion so that fuel consumption can be optimized.

As shown in Table 1, the variation in mixed gas composition results in

fluctuation in CV leading to the variation in combusting character. To circumvent this issue, CV for every instance has been calculated based on the basic governing equation of combustions as given in Eq. 1.

$$\text{Calorific Value} = \sum_{i=1}^{n} \text{Volume \% of Component } i \times \text{Calorific Value of Component } i \quad (1)$$

where:

n: Number of gas Components;

Volume % of Component i: Volume percentage of gas component i;

Calorific Value of Component i: Calorific value of gas component i in energy units.

Table 1. Variation in mixed gas composition.

Properties	Unit	BF Gas	Coke Oven Gas	LD Gas
Carbon Dioxide	% by Vol	17 - 19	2.8 - 3.2	13 - 15
Oxygen	% by Vol	0.2 - 1.0	0.2 - 1.0	0.4 - 1.2
Unsaturated Hydrocarbon	% by Vol	Nill	2.0 - 3.0	Nill
Carbon Monoxide	% by Vol	21 - 25	8.8 - 9.0	50 - 70
Hydrogen	% by Vol	3.0 - 6.0	53 - 55	2 - 3
Methane	% by Vol	Nill	21 - 23	Nill
Nitrogen	% by Vol	Balance	Balance	Balance

Figure 4 shows hourly variation of CV for a single day, ranging from 2000 Gcal to 2300 Gcal. However, mixed gas property depends upon various other factors *i.e.*, gas temperature, density, specific heat, and viscosity. Figure 5 shows the property variation of same flue gas with respect to temperature. Hence, variation in CV has been considered for the present model to achieve accurate prediction of heat transfer.

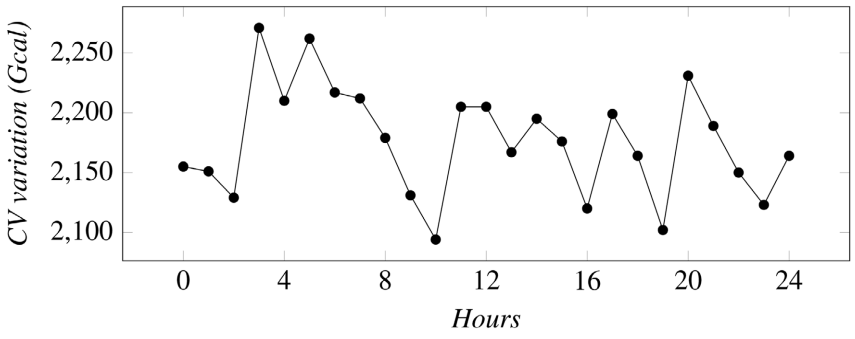

Figure 4. Hourly variation in CV for a single day.

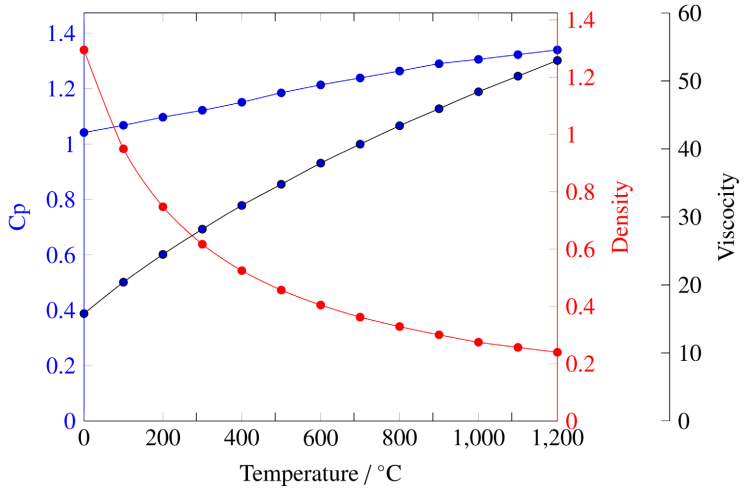

Figure 5. Property variation of flue gas with temperature.

2.3. Air-Fuel Ratio Optimization

A complete combustion process of mixed gas with preheated air with a base value ratio namely a stoichiometric combustion, generates desired heat for reheating the stock. To achieve the optimum ratio considering the variation in CV for such a huge furnace with multiple zones is a key challenge for a steel plant. Kangvanskol et al. has described in his article that, for achieving a stoichiometric combustion is practically not possible due to the limitation of the air and fuel mixing, variation in CV and combustion time [16] [17]. Hence, optimum excess air λ must be provided for the complete combustion of unburned fuel inside the furnace. The percentage of excess air can be measured based on following Eq: 2.

$$\lambda = \frac{AF_{actual}}{AF_{stoic}} \tag{2}$$

where, AF_{actual} refers to actual air-fuel ratio and AF_{stoic} refers to the base value ratio or stoichiometric air-fuel ratio. In industrial practice, input of excess air is controlled based on the measurement of online oxygen analyzer. It usually operates at the flue gas exit to obtain the actual volume percentage of oxygen in it and apparently maintained under 3 vol%. The variation in vol% of produced flue gas depends on the percentage of input excess air. **Figure 6** shows a typical linear correlation in terms of vol% between combustion air (input air), excess air and flue gas. This means supply of excessive air generates high volume of flue gas, leading to more heat content. This heat is lost while the flue gas leaves the system, which basically leads to lower efficiency of furnace. There are other various disadvantages of additional excess air into the system, such as a) localized cooling of heated zone as well as stock, b) excess gas consumption during maintaining of air-fuel ratio, c) reduction in flame temperature, and d) more carbon footprint. In this present study, the input of excess air percentage has been optimized depending upon the varying CV of mixed gas and stoichiometric air-fuel ratio. A

feedback model has been introduced for each zone of the furnace, which measures the difference of input air-fuel ratio with respect to stoichiometric ratio over varying CV for each and every instance. The output of feedback model controls the system in such a manner that both ratios should be nearer to each other. Figure 7 shows a complete algorithm of the above-mentioned feedback model. However, due to industrial environment and practical point of view, a relaxation of 5% - 10% in variation between two ratios has been incorporated into the model. This relaxation percentage also follows a comparison node where the relaxed percentage is decided upon the best time performance of furnace. The decision node controls the adjustment of input air-fuel ratio based on feedback of all the input and resulted nodes.

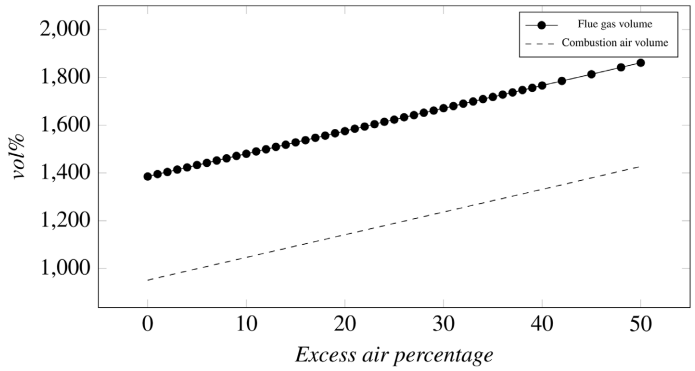

Figure 6. Variation in flue gas vol% based on input excess air for mixed gas.

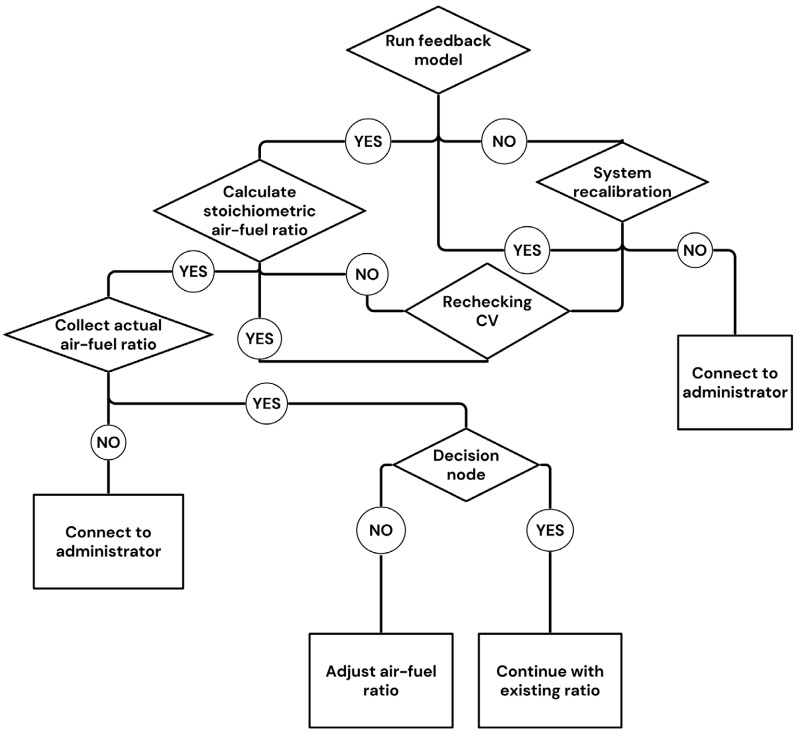

Figure 7. Computational flowchart of the algorithm of feedback model.

2.4. Heat and Mass Balance of Tunnel Type Continuous Furnace and Attached Recuperator

The produced heat due to combustion of fuel, undergoes to industrial process typically leaves the system as flue gas, which contains maximum percentage of heat Q_f. The remaining heat is transferred to the atmosphere as various losses like furnace wall losses or skin losses Q_s, opening losses during stock in and out (door opening) Q_d and cooling system losses (water is used as coolant in the skids/rolls/doors usually) Q_w [18]. The quantity of consumed heat Q_c by the stock can be estimated from the following equation Eq: 3.

$$Q_c = mC_p\left(T_2 - T_1\right) \tag{3}$$

where, Q_c is the quantity of heat in kJ, m is the mass of the material in kg, C_p is the mean specific heat, T_1 and T_2 are the initial and final desired temperature of the charge. Similarly, rate of heat losses due to cooling system Q_w as well as rate of heat transfer from the walls or skins of the furnace Q_s can also be estimated from the equations Eq: 3 and Eq: 4 respectively. The radiative heat loss due to the door opening Q_d can be obtained with the help of total radiation factor chart [19].

$$Q_s = -k \cdot A \cdot \frac{\mathrm{d}T}{\mathrm{d}x} \tag{4}$$

where, k is the thermal conductivity in watt/m-K, A is the area of the furnace walls in m^2 and $\mathrm{d}T/\mathrm{d}x$ is the variation in temperature gradient with respect to wall thickness. According to the law of energy conservation, the total input heat H must be equal to the sum of consumed heat Q_c by the stock and the sum of various heat losses Eq: 5.

$$H = Q_c + \sum_{i=1}^{n} Q_s + \sum_{j=1}^{p}\left(Q_w + Q_d\right) + Q_f \tag{5}$$

where,

n: Number of furnace walls exposed to atmosphere.

p: Number of skids/rolls/doors

From the Eq: 5 it is obvious that to increase the efficiency of a reheating furnace, heat losses must be as minimum so that the maximum input heat can be utilized for heating the charged material. In the present study, it has been considered that the material of furnace wall and charging stock both are individually homogeneous and isotropic. Due to door opening at furnace entry as well as furnace exit, heat loss does not vary significantly while a slab enters the furnace or leaves the soaking zone. This is because of fixed door opening height. Note that subsection 2.1, where the furnace dimension and operation details has been described also contains detail of roll cooling system. The heat losses also take place due to the roll cooling where water is used as cooling medium. In this case ΔT has been calculated using Eq: 3 based on water inlet temperature (T_1) and outlet temperature (T_2). Here, C_p the specific heat of water and m is the mass flow rate of water. In

general, Erosion of refractory lining on the outer surface of the rolls results in additional heat loss from the furnace. This can be evident from the pattern of ΔT.

Efficiency of recuperator η_{recup} is an important feature which has a relation with thermal efficiency η_C of the reheating furnace. A higher η_{recup} indicates higher heat recovery from the flue gas exit, which is typically used for preheating combustion air or input mixed gas or both [20] [21]. In the referenced article, authors have explained how the thermal efficiency η_C depends on enthalpy released by combustion, furnace ability to extract energy from combustion of air-fuel mix and recuperator efficiency η_{recup}. The volumetric thermal capacity $s(T)$ of flue gas and combustion air $a(T)$ can be measured from the Eq: 6 and Eq: 7.

$$s(T) = V_{flue} \times \rho_{flue} \times C_{p(flue)} \times T \tag{6}$$

where, $s(T)$ is the thermal capacity of flue gas at temperature T in KJ, V_{flue} is the flue gas volume in m^3, ρ_{flue} is the flue gas density and $C_{p(flue)}$ is the specific heat of flue gas at same temperature.

$$a(T) = V_{air} \times \rho_{air} \times C_{p(air)} \times T \tag{7}$$

where, $a(T)$ is the thermal capacity of combustion air at temperature T in KJ, V_{air} is the combustion air volume in m^3, ρ_{air} is the combustion air density and $C_{p(air)}$ is the specific heat of combustion air at same temperature. Using Eq:6 and Eq:7 the thermal efficiency η_C of tunnel furnace and efficiency of each recuperator η_{recup} has been estimated from Eq:8 and Eq:9 respectively.

$$\eta_C = \sum_{sec=1}^{n} \frac{10^6 - (\theta_1 - T_{ambient}) \times s(T) + (T_{combair} - T_{ambient}) \times a(T)}{n \times 10^6} \times 100\% \tag{8}$$

$$\eta_{recup} = \frac{a(T) \times (T_{combair} - T_{ambient})}{s(T) \times V_{frac} \times (\theta_1 - \theta_2)} \tag{9}$$

where, n is the number of sections inside the furnace, $T_{combair}$ and $T_{ambient}$ are the combustion air temperature and ambient temperature in ˚C, V_{frac} is the volume fraction of flue gas V_{flue} and combustion air V_{air}, θ_1 and θ_2 are the flue gas temperature before and after the recuperator respectively in ˚C. The overall heat loss in terms of percentage due to flue gas has been estimated from the following Eq:10.

$$Q_f = 100\% - \eta_C \tag{10}$$

where, Q_f heat loss due to flue gas in %. For estimating the real time furnace efficiency and heat losses, all the above equations have been integrated as additional node to the model. A parallel activity of model, during furnace runtime has been scheduled for each furnace and model output is visualized invariably to mitigate the abnormal behavior of furnace. It is worthy to mention another important aspect by Seong *et al.* [22] where authors have explained that high temperature corrosion on heat exchanger pipe of a recuperator is a very serious problem

resulting in degradation of recuperator performance. This high temperature corrosion predominantly occurs due to oxidation, sulfidation and presence of molten salt. To improve the consistency of recuperator performance, the authors have suggested a Cr3C2-NiCr coating in carbide form, and Ni-45Cr-4Ti as an alloy coating for heat exchanger pipes of recuperator. The suggested coating has an excellent resistivity of corrosion at high temperature.

3. Results and Discussion

The whole furnace operation is controlled automatically by Level—2 or L2 systems which processes millions of time series process data to control the furnace temperature in set regime. Before implementation of the integrated model at furnace, a detailed study has been carried out for energy efficiency and heat balance for existing conditions based on L2 processed data. Figure 8 shows a daily average trend of actual and stoichiometric air-fuel ratio for a period of two months. In this figure, each blue dot refers to a single day average value of air-fuel ratio which is quite higher than the recommended air-fuel ratio for the same day denoted by red dots. It is worth to note that the recommended air-fuel ratio is measured based on the average CV variation for the same day with 5% - 10% relaxation. Therefore, from the figure, it can be inferred that either the furnace L2 process control was unable to follow the command, or the input air-fuel ratio given by the operator, namely Operator ratio was not optimized. In order to further analyze, a significant variation in input air-fuel ratio has been observed with respect to variation in CV for both the furnaces.

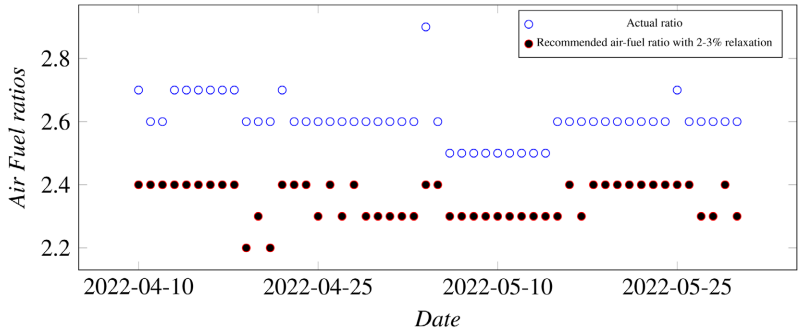

Figure 8. Daily average of actual and recommended air-fuel ratio by model.

Figure 9(a) shows, at a given CV, input air-fuel ratio was varying in a wide range of 2.4 - 2.9 which is undesirable. Practically, the ideal variation should be in a narrow band and distributed in both side of recommended ratio. However, in this study, the variation is one sided for the existing condition. After implementation of the feedback model Figure 7, the input air-fuel ratio has been auto restricted and is compelled to follow the recommended air-fuel ratio given by the model. This resulted in production of lesser flue gas volume leading to lesser heat

loss. As shown in Figure 9(b), a narrow and almost evenly distributed input air-fuel ratio at both side of recommended ratio can be seen. This indicates a significant improvement in input excess air percentage into the furnace.

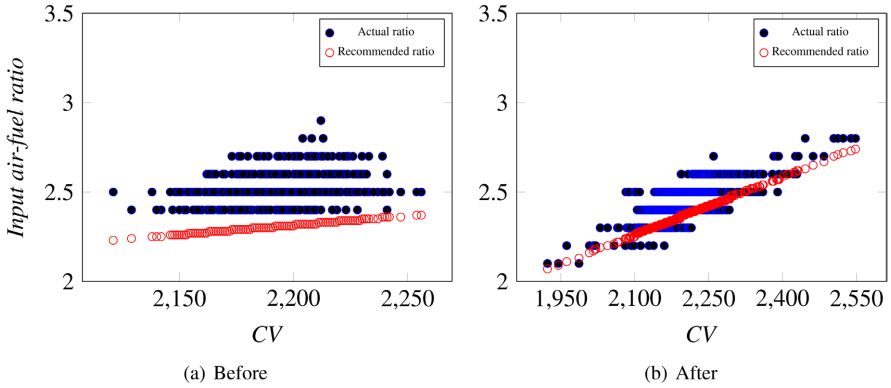

(a) Before (b) After

Figure 9. Variation of input air-fuel ratio before and after implementation of model.

Refer subsection 2.4 where a details of heat and mass balance has been explained and basically, this can be represented by a typical Sankey diagram, as shown in Figure 10. The total heat input and percentage fractions of heat losses by various medium over total heat loss has been visualized along with stock entry and exit temperature during furnace runtime for a given CV, air-fuel ratio and throughput of the furnace. Based on the real time visualization of various heat losses, necessary action is taken to improve the energy efficiency of the tunnel furnace.

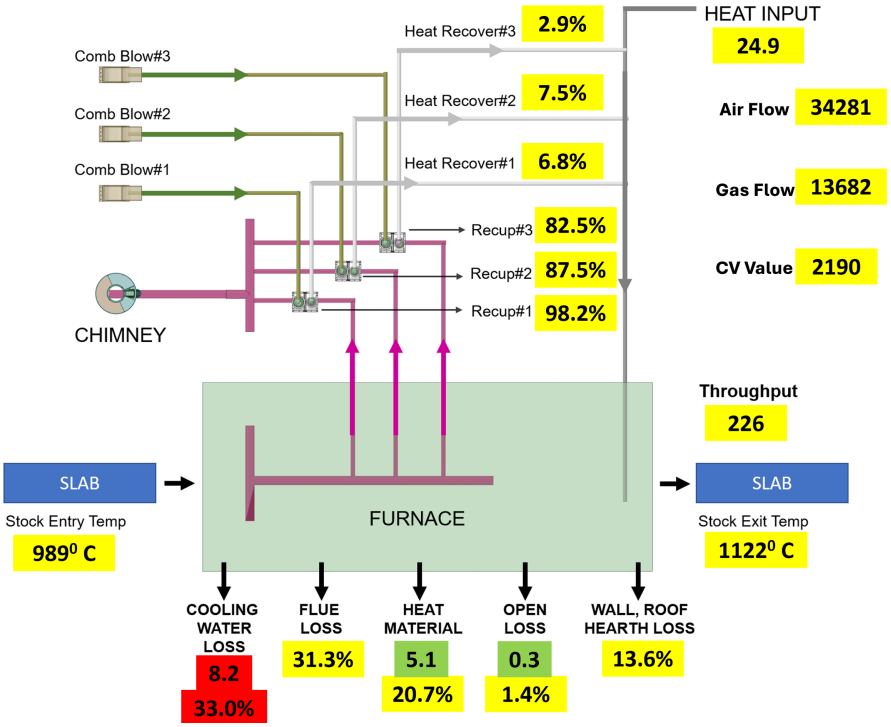

Figure 10. Sankey diagram of tunnel type furnace.

The above sanky diagram also shows the efficiency of recuperators based on heat recovery from the exit flue gas. The efficiency over a time period is a good indicator for recuperator health condition.

After taking all corrective measures and deployment of the integrated model has resulted in a significant improvement in furnace efficiency which has led to a significant reduction in energy consumption by 14.63%.

Figure 11 shows a long-term trend of monthly fuel consumption with respect to production output (in Gcal/T). From the above figure, two-fold improvement can be observed from September 2022 and onwards since the inception of the model leading to optimization of air-fuel ratio. The second improvement can be seen after April 2023 onwards, where the action has been taken to minimize heat losses based on the output of real time visualization for both the furnaces. In addition, this visualization toolbox of the model has enabled following corrective actions based on anomalies in the trend: (a) optimized cycle time for embedded refractory lining of rolls (b) installation of pyrometer near furnace doors, roof and side walls for capturing real time average heat losses (c) clearing the blockage of gas pipeline (d) calibration of thermocouple reading etc. The above corrective actions have also helped to boost the furnace efficiency further.

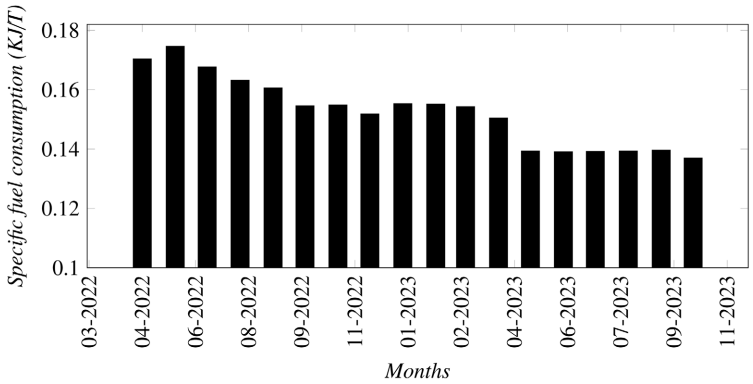

Figure 11. A combined chart of monthly specific fuel consumption for furnace A and furnace B.

4. Conclusion

An integrated furnace model based on heat and mass balance has led to development of a feedback control-based model to improve the efficiency of a furnace. The model enables real time visualization as well as it provides actionable process parameters to improve the efficiency of a furnace. Overall, it can be stated that a simplified approach of past data analytics combined with optimized input air-fuel ratio and real time visualization of heat and mass balance of a tunnel type continuous furnace can improve the energy efficiency and reduce excessive fuel consumption. This model has possibility to be adapted for numerous types of furnaces in a quick way.

Acknowledgements

We wish to express our deep sense of gratitude to the entire team at LD3-TSCR, Tata Steel Ltd. Jamshedpur for their support during this study.

Conflicts of Interest

The authors declare no conflicts of interest regarding the publication of this paper.

References

[1] Jang, J. and Huang, J. (2015) Optimization of a Slab Heating Pattern for Minimum Energy Consumption in a Walking-Beam Type Reheating Furnace. *Applied Thermal Engineering*, **85**, 313-321. https://doi.org/10.1016/j.applthermaleng.2015.04.029

[2] Zhang, C., Ishii, T. and Sugiyama, S. (1997) Numerical Modeling of the Thermal Performance of Regenerative Slab Reheat Furnaces. *Numerical Heat Transfer*, *Part A*: *Applications*, **32**, 613-631. https://doi.org/10.1080/10407789708913909

[3] Jong Gyu Kim, Kang Y. Huh, Il Tae K, (2000) Three-Dimensional Analysis of the Walking-Beam-Type Slab Reheating Furnace in Hot Strip Mills. *Numerical Heat Transfer*, *Part A*: *Applications*, **38**, 589-609. https://doi.org/10.1080/104077800750021152

[4] Huang, M., Hsieh, C., Lee, S. and Wang, C. (2008) A Coupled Numerical Study of Slab Temperature and Gas Temperature in the Walking-Beam-Type Slab Reheating Furnace. *Numerical Heat Transfer*, *Part A*: *Applications*, **54**, 625-646. https://doi.org/10.1080/10407780802289475

[5] Hsieh, C., Huang, M., Lee, S. and Wang, C. (2010) A Numerical Study of Skid Marks on the Slabs in a Walking-Beam Type Slab Reheating Furnace. *Numerical Heat Transfer*, *Part A*: *Applications*, **57**, 1-17. https://doi.org/10.1080/10407780903529308

[6] Han, S.H., Chang, D. and Kim, C.Y. (2010) A Numerical Analysis of Slab Heating Characteristics in a Walking Beam Type Reheating Furnace. *International Journal of Heat and Mass Transfer*, **53**, 3855-3861. https://doi.org/10.1016/j.ijheatmasstransfer.2010.05.002

[7] Gu, M., Chen, G., Liu, X., Wu, C. and Chu, H. (2014) Numerical Simulation of Slab Heating Process in a Regenerative Walking Beam Reheating Furnace. *International Journal of Heat and Mass Transfer*, **76**, 405-410. https://doi.org/10.1016/j.ijheatmasstransfer.2014.04.061

[8] Morgado, T., Coelho, P.J. and Talukdar, P. (2015) Assessment of Uniform Temperature Assumption in Zoning on the Numerical Simulation of a Walking Beam Reheating Furnace. *Applied Thermal Engineering*, **76**, 496-508. https://doi.org/10.1016/j.applthermaleng.2014.11.054

[9] Emadi, A., Saboonchi, A., Taheri, M. and Hassanpour, S. (2014) Heating Characteristics of Billet in a Walking Hearth Type Reheating Furnace. *Applied Thermal Engineering*, **63**, 396-405. https://doi.org/10.1016/j.applthermaleng.2013.11.003

[10] Han, S.H., Baek, S.W. and Kim, M.Y. (2009) Transient Radiative Heating Characteristics of Slabs in a Walking Beam Type Reheating Furnace. *International Journal of Heat and Mass Transfer*, **52**, 1005-1011. https://doi.org/10.1016/j.ijheatmasstransfer.2008.07.030

[11] Yang, B.Y., Wu, C.Y., Ho, C.J. and Ho, T.Y. (1995) A Heat Transfer Model for Skid Mark Formation on Slab in a Reheating Furnace. *Journal of Materials Processings and Manufacturing Science*, **3**, 277-295.

[12] Han, S.H. and Chang, D. (2012) Optimum Residence Time Analysis for a Walking Beam Type Reheating Furnace. *International Journal of Heat and Mass Transfer*, **55**, 4079-4087. https://doi.org/10.1016/j.ijheatmasstransfer.2012.03.049

[13] Fan, H., Feng, J., Hu, W., Li, W. and Gao, J. (2021) Effect of Excess Air Coefficient on the Combustion Characteristics of a Multi-Stage Dual Swirl Burner. *Journal of Physics*: *Conference Series*, **2009**, Article ID: 012076. https://doi.org/10.1088/1742-6596/2009/1/012076

[14] Han, S.H., Lee, Y.S., Cho, J.R. and Lee, K.H. (2018) Efficiency Analysis of Air-Fuel and Oxy-Fuel Combustion in a Reheating Furnace. *International Journal of Heat and Mass Transfer*, **121**, 1364-1370. https://doi.org/10.1016/j.ijheatmasstransfer.2017.12.110

[15] Zhang, K., Zheng, Z., Feng, L., Su, J. and Li, H. (2023) A Byproduct Gas Distribution Model for Production Users Considering Calorific Value Fluctuation and Supply Patterns in Steel Plants. *Alexandria Engineering Journal*, **76**, 821-834. https://doi.org/10.1016/j.aej.2023.06.063

[16] Kangvanskol, K. and Tangthieng, C. (2014) An Energy Analysis of a Slab Preheating Chamber for a Reheating Furnace. *Engineering Journal*, **18**, 1-12. https://doi.org/10.4186/ej.2014.18.2.1

[17] Moran, M.J. and Shapiro, H.N. (2004) Reacting Mixtures and Combustion. *Fundamentals of Engineering Thermodynamics*, **13**, 661-664.

[18] Chakravarty, K. and Kumar, S. (2020) Increase in Energy Efficiency of a Steel Billet Reheating Furnace by Heat Balance Study and Process Improvement. *Energy Reports*, **6**, 343-349. https://doi.org/10.1016/j.egyr.2020.01.014

[19] Trinks, W., Mawhinney, M.H., Shannon, R.A., Reed, R.J. and Garvey, J.R. (2004) Industrial Furnaces Book with chapter Furnace, Kiln and Oven Heat Losses. 6th Edition, John Wiley & Sons, Inc. Hoboken, New Jersey, 189-191.

[20] Steinboeck, A., Wild, D. and Kugi, A. (2013) Energy-Efficient Control of Continuous Reheating Furnaces. *IFAC Proceedings Volumes*, **46**, 359-364.

[21] Adeniji, T.A. and Waheed, M.A. (2021) Evaluation of the Energy Efficiency of an Aluminum Melting Furnace for a Nigerian Cast-Coiled Plant. *Fuel Communications*, **9**, Article ID: 100027. https://doi.org/10.1016/j.jfueco.2021.100027

[22] Seong, B.G., Hwang, S.Y. and Kim, K.Y. (2000) High-temperature Corrosion of Recuperators Used in Steel Mills. *Surface and Coatings Technology*, **126**, 256-265. https://doi.org/10.1016/s0257-8972(00)00523-5